ELSEVIER

International Journal of Refrigeration 26 (2003) 442–451

REVUE INTERNATIONALE DU FROID
INTERNATIONAL JOURNAL OF
refrigeration

www.elsevier.com/locate/ijrefrig

Refrigerant charge, pressure drop, and condensation heat transfer in flattened tubes

M.J. Wilson[a], T.A. Newell[a,*], J.C. Chato[a], C.A. Infante Ferreira[b]

[a]*Department of Mechanical and Industrial Engineering, University of Illinois at Urbana-Champaign 140 MEB, MC-244, 1206 W. Green St., Urbana IL 61801, USA*

[b]*Delft University of Technology, Lab. for Refrigeration and Indoor Climate Control Mekelweg 2, 2628 CD Delft, The Netherlands*

Received 9 January 2002; received in revised form 28 August 2002; accepted 2 September 2002

Abstract

Horizontal smooth and microfinned copper tubes with an approximate diameter of 9 mm were successively flattened in order to determine changes in flow field characteristics as a round tube is altered into a flattened tube profile. Refrigerants R134a and R410A were investigated over a mass flux range from 75 to 400 kg m^{-2} s^{-1} and a quality range from approximately 10–80%. For a given refrigerant mass flow rate, the results show that a significant reduction in refrigerant charge is possible. Pressure drop results show increases of pressure drop at a given mass flux and quality as a tube profile is flattened. Heat transfer results indicate enhancement of the condensation heat transfer coefficient as a tube is flattened. Flattened tubes with an 18° helix angle displayed the highest heat transfer coefficients. Smooth tubes and axial microfin tubes displayed similar levels of heat transfer enhancement. Heat transfer enhancement is dependent on the mass flux, quality and tube profile.

Keywords: Refrigerating circuit; Refrigerant; Charge; Heat transfer; Condensation; Tube; Geometry

Charge en frigorigène, chute de pression et transfert de chaleur lors de la condensation à l'intérieur de tubes plat

Mots clés : Circuit frigorifique ; Frigorigène ; Charge ; Transfert de chaleur ; Condensation ; Tube ; Géométrie

1. Introduction

This paper summarizes important results from an investigation of flattened refrigerant tubes. The purpose of this investigation is an examination of refrigerant behavior (pressure drop, heat transfer coefficient, void fraction) in flattened copper passageways. This study is motivated by the desire to explore the advantages and disadvantages of refrigerant flow through small copper passageways. Potential advantages of flattened tube profiles are reduced air-side pressure drop and increased air-side heat transfer.

Twelve different channel configurations are investigated using two refrigerants, R134a and R410A, under condensation conditions at 35 °C. The tubes used are a smooth tube and two microfin tubes, one with an 18° helix angle and one with a 0° helix angle (axially finned). The tubes are initially round with a 9.52 mm (3/8″) outer diameter, and 8.91 mm (0.351″)

* Corresponding author. Tel.: +1-217-333-1655; fax: +1-217-333-1942.

E-mail addresses: t-newell@uiuc.edu (T.A. Newell).

0140-7007/03/$30.00
doi:10.1016/S0140-7007(02)00157-3

Nomenclature

A_s	surface area, m^2
D	diameter, m
D_h	hydraulic diameter, m
e	tube roughness, m
EF	enhancement factor
f	friction factor
Fr	Froude number
Ft	Froude rate parameter
g	gravity, 9.81 m s^{-2}
G	mass flux, kg m^{-2} s^{-1}
h	heat transfer coefficient, Wm^{-2} K^{-1}
h_{fin}	fin height, m
P	perimeter, m
Re	Reynolds number
X_{tt}	Lockhart Martinelli parameter
x	quality
α	void fraction
β	helix angle
ϕ	two phase multiplier
ρ	density, kg m^{-3}
μ	viscosity, kg m^{-1} s^{-1}

Subscripts

v	vapor
l	liquid

inner base diameter. The tubes are successively flattened into an oblong shape with inside heights of 5.74 mm, 4.15 mm, 2.57 mm, and 0.974 mm (0.226″, 0.163″, 0.101″, 0.0383″) as shown in Figs. 1 and 2. The corresponding hydraulic diameters are 7.79 mm, 6.37 mm, 4.40 mm, and 1.84 mm. The microfin tubes contain 60 fins around the tube perimeter with approximate fin height of 0.2 mm. The microfins increase the internal surface area by 60% over the smooth tube.

2. Experimental facility and procedures

Fig. 3 is a schematic of the experimental apparatus used in this study. A magnetically coupled, variable speed pump is used to circulate liquid refrigerant. The pump requires no lubricant, leaving the refrigerant uncontaminated. The mass flow rate of the refrigerant is measured using a Coriolis-type mass flow meter. The refrigerant passes through the pre-heater that consists of a series of electric heater strips. The pre-heater is used to condition the flow from sub-cooled liquid to the desired two-phase quality. Two-phase refrigerant then enters the test section. After the test section, the refrigerant is cooled using a water-cooled condenser. The refrigerant then enters a receiver tank to separate the liquid from any remaining vapor.

The test sections are horizontally mounted 1.22 m (48″) long copper tubes. Pressure taps are soldered at the inlet and outlet, and are attached to a differential pressure transducer and an absolute pressure transducer. A void fraction tap is also soldered onto the test section to allow for the extraction of refrigerant from the test section. At the test section inlet and outlet are two ball valves that can be simultaneously closed for void fraction sampling.

To flatten the test section tube, the 9.525 mm (3/8″) diameter round tube is placed between two 6.35 mm (1/4″) thick by 25.4 mm (1″) wide by 1.2 m long copper bars. A spacer, with heights of 6.35 mm, 4.76 mm, 3.18 mm, or 1.59 mm (1/4″, 3/16″, 1/8″, or 1/16″) is then placed between the two copper bars. The two copper bars are then tightened to together using a series of bolts spaced approximately 25.4 mm apart along the test section length. The outside tube height of the test section is determined by the spacer. Copper coolant tubes are soldered to the outside surface of the copper bars. Water is passed through the coolant tubes on top and on bottom of the copper bars in a counter flow configuration. The water is able to remove up to 400 W from the refrigerant.

Four wall-mounted thermocouples are placed every 0.3 m (9.6″) at four stations along the test section tube length to measure the tube wall temperature. The four

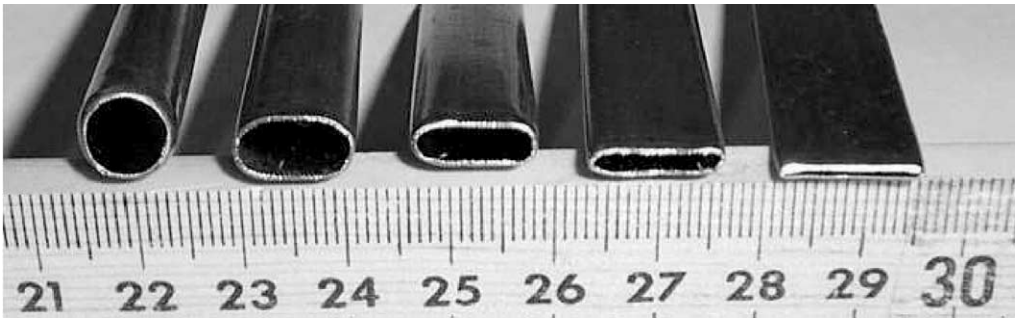

Fig. 1. Photograph of flattened tube cross sections.

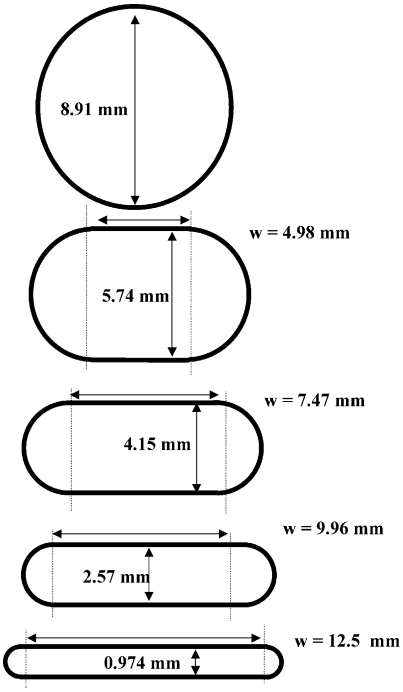

Fig. 2. Dimensions of flattened tube cross-sections.

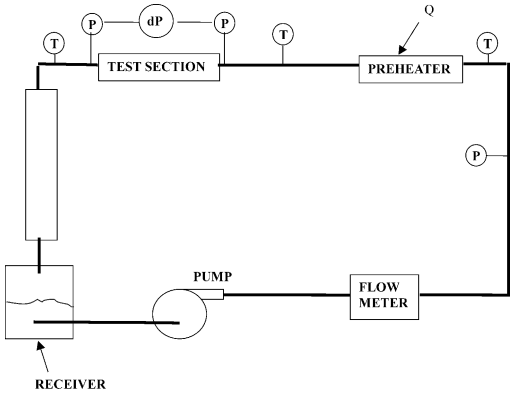

Fig. 3. Schematic of refrigerant test loop.

thermocouples at each station are mounted on the top, bottom, and opposing sides of the tube.

Experiments were performed using both R134a and R410A at an inlet temperature of 35 °C. The mass flux was generally varied from 75 kg m^{-2} s^{-1} to 400 kg m^{-2} s^{-1}. The inlet quality was varied from 10% up to 80%. During heat transfer tests, the inlet and outlet quality variations of the test section were between 0.05 to 0.5. The average of the inlet and outlet quality has been used to define the quality in the figures presented. The greatest quality changes occurred in the flattest test sections where refrigerant mass flow rates were smallest.

The test section tubes had a nominal outside diameter of 9.53 mm (3/8″) with a wall thickness of 0.3 mm (0.012″). The fin height on the microfin tubes was 0.2 mm (0.008″) with a total of 60 fins. The helical and axial finned tubes had identical cross-section geometry. The tubes were successively flattened from an initial internal diameter of 8.91 mm (0.351″) to heights of 5.74 mm, 4.15 mm, 2.57 mm, and 0.974 mm (0.226″, 0.163″, 0.101″, 0.0383″). In the microfin tubes, this is the distance from the base of the fin to the base of fin on the other side of the tube.

The refrigerants tested in this experiment represent a mid-pressure refrigerant (R134a) and a high-pressure refrigerant (R410A). It is believed that refrigerants with vapor pressures between these limits (e.g., R22 and R404A) and similar liquid thermal conductivity and viscosity will behave in a manner somewhere between the R134a and R410A results.

The void fraction measurement technique is one that has been commonly used by others [1]. First, the test section inlet condition must be set to the desired temperature, quality, and mass flow rate. The valves on both sides of the test section are closed simultaneously and a by-pass line of the refrigerant flow circuit is opened. A valve on the void fraction tap connecting the test section to a receiver tank is opened, allowing refrigerant to flow out of the test section and into the tank. The tank is cooled in an ice bath. After the mass has migrated to the receiver tank, the temperature and pressure of the test section are recorded and the void fraction tap valve is closed.

The amount of vapor mass left in the test section is calculated and the mass collected in the receiving tank is weighed. The specific volume of the test section refrigerant is determined by dividing the test section volume by the refrigerant mass. All thermodynamic properties are evaluated at the test section inlet condition of 35 °C.

The most common source of error in the void fraction experiment is refrigerant leaks. Refrigerant can leak from loose fittings and improperly soldered joints, resulting in lower than actual amounts of mass in the receiving tank. Also, leaks across the shutoff valves can add refrigerant mass to the receiving tank. This method gives consistent mass readings to within 0.5 gram (usually less than 5% of test section mass).

Heat transfer coefficients are determined by measuring the temperature difference between the tube wall and refrigerant with a measured heat transfer. The refrigerant temperature is measured at the inlet and outlet of the test section. The "local" refrigerant temperature at each thermocouple station is linearly interpolated from the inlet and outlet refrigerant temperatures. The heat transfer is determined from the water circulated through the cooling circuits bonded to the copper bars. The water mass flow rate in the cooling circuit is measured by the "bucket-stopwatch" method.

Instrumentation includes thermocouples, differential and absolute pressure transducers, mass flow meters, and watt-hour transducers. Type T thermocouples were used to measure temperature. The uncertainty of these thermocouples was measured to be ±0.25 °C. The uncertainty of the absolute pressure transducers was calculated to be ±35 kPa (5 psi). The range of the differential pressure transducer is 0–35 kPa (0–5 psi), with an accuracy of ±0.4 kPa. Two watt-hour transducers were used to measure the pre-heater inlet power. The accuracy of these transducers were individually calculated by single-phase liquid flow energy balances to be within 3%. The refrigerant mass flow meter was found to be accurate to within 3% by comparison with a bucket-stopwatch calibration. An error analysis [2] indicates that quality can be calculated to within 10% and the mass flux to within ±5 kg m^{-2} s^{-1}. The void fraction can be measured accurately to within 8%, pressure drop to within 0.4 kPa, and heat transfer coefficient to within 20%.

3. Void fraction results

Two-phase refrigerant void fraction data was collected for each of flattened tube profiles for refrigerants R134a and R410A. The quality was varied from 10% to 80% and the mass flux ranged from 75 to 400 kg m^{-2} s^{-1}. The data was compared to a correlation given by Wilson et al. [2] in which the void fraction is dependent on the Lockhart Martinelli parameter (X_{tt}) and a modified Froude Number (Ft).

$$X_{tt} = \left(\frac{1-x}{x}\right)^{0.9}\left(\frac{\rho_v}{\rho_l}\right)^{0.5}\left(\frac{\mu_l}{\mu_v}\right)^{0.1} \quad (1)$$

$$\mathrm{Ft} = \left[\frac{x^3 G^2}{\rho_v^2 g D(1-x)}\right]^{\frac{1}{2}} \quad (2)$$

$$\alpha = (1 + a/Ft + b\cdot X_{tt})^n \quad (3)$$

New constants (a,b,n) were used to update this correlation for flattened tubes. These constants appear in Tables 1 and 2. Different constants are used for different flow regimes [if the tube height is greater or less than 2.5 mm, or if ($X_{tt}+1/\mathrm{Ft}$) is greater than or less than 2].

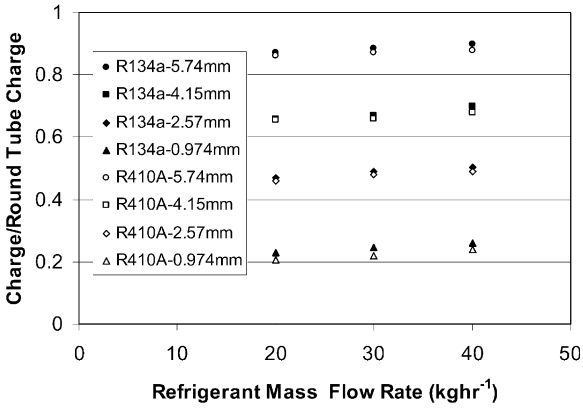

Fig. 4. Relative changes in refrigerant charge for flattened tubes with refrigerants R134a and R410A.

The main effect of flattening a tube at a constant mass flow rate is the increased vapor velocity. The bulk of a tube's cross section at qualities greater than 0.2 is vapor. When a tube's cross section is reduced in half, the vapor velocity is essentially doubled, which is a quadrupling of the vapor's kinetic energy. This increase in vapor kinetic energy results in a higher shearing of the liquid layer, thinning the liquid phase, which reduces the mass in the tube.

Charge requirements of a heat exchanger can be determined by numerical integration of the void fraction relation over a quality range of interest. Fig. 4 displays the effect of flattening the tube on refrigerant charge ratio. The ratio of charge in a flattened tube to charge in a round tube has little dependence on mass flux or refrigerant type. The total charge, however, will depend on both mass flux and refrigerant. The ratio is highly dependent on tube height.

4. Pressure drop results

The experimental pressure drop for the test sections was compared against pressure drop correlations found in the published literature [2]. For flattened tubes, the

Table 1
Void fraction correlation constants for tube heights greater than 2.5 mm

Tube	$X_{tt}+1/\mathrm{Ft}$	a	b	n
Smooth	<2.00	1.84	3.11	−0.21
	>2.00	0.5	1.2	−0.35
18 Helix	<2.00	5.80	8.60	−0.16
	>2.00	1.50	2.70	−0.31
0 Helix	<2.00	1.38	3.30	−0.26
	>2.00	2.26	2.50	−0.26

Table 2
Void fraction correlation constants for tube heights of 0.974 mm

Tube	$X_{tt}+1/\mathrm{Ft}$	a	b	n
Smooth	<2.00	1.84	3.11	−0.21
	>2.00	0.5	1.2	−0.35
18 Helix	<2.00	5.80	8.60	−0.16
	>2.00	1.50	2.70	−0.31
0 Helix	<2.00	1.38	3.30	−0.26
	>2.00	2.26	2.50	−0.26

diameter length scale was chosen to be the hydraulic diameter of the smooth tube ($D_h = 4A/P$). Two correlations presented in this work for illustrative purposes are the models by Jung and Radermacher [3] and Souza et al. [4]. These models are both "two-phase multiplier" type models that are functions of the Lockhart Martinelli parameter.

The Jung and Radermacher [3] model uses the "liquid only" formulation. The liquid only formulation treats all refrigerant mass flow as if it is in the liquid phase. That is, the single phase pressure gradient is determined from a suitable single phase friction factor expression with all refrigerant mass flow considered as liquid. The two-phase multiplier is given by the relation:

$$\phi_{lo}^2 = 12.82 \cdot X_{tt}^{-1.47}(1-x)^{1.8} \tag{5}$$

And the two-phase pressure gradient is determined from:

$$\frac{dP}{dz})_f = \phi_{lo}^2 \left(\frac{dP}{dz}\right)_{lo} \tag{6}$$

The Souza et al. [4] correlation is based on the "liquid" two-phase multiplier. In this case, only that liquid mass for a given quality is used is used for determining the single phase pressure gradient. This model uses a simple Froude number expression to differentiate between stratified and annular flow regions as seen in the relations below.

$$\phi_l^2 = 1.376 + c_1 X_{tt}^{-c_2} \tag{7}$$

$$c_1 = 4.172 + 5.48\mathrm{Fr}_l - 1.564\mathrm{Fr}_l^2 \mathrm{Fr}_l < 0.7 \tag{8}$$

$$c_1 = 7.242\mathrm{Fr}_l > 0.7 \tag{9}$$

$$c_2 = 1.773 - 0.169\mathrm{Fr}_l \ \mathrm{Fr}_l < 0.7 \tag{10}$$

$$c_2 = 1.655\mathrm{Fr}_l > 0.7 \tag{11}$$

$$\frac{dP}{dz})_f = \phi_l^2 \left(\frac{dP}{dz}\right)_l \tag{12}$$

where the liquid Froude number is defined as: $\mathrm{Fr}_l = \frac{G}{\rho_l \sqrt{gD}}$ To account for the effects of microfins, the Cavallini et al. [5] roughness ratio is used in conjunction with the Colebrook [6] friction factor relation.

$$\frac{e}{D} = 0.18\left(\frac{h_{fin}}{D_h}\right)\left(\frac{1}{0.1+\cos\beta}\right) \tag{13}$$

$$\frac{1}{f^{0.5}} = -2.0 \cdot \log_{10}\left(\frac{e/D}{3.7} + \frac{2.51}{\mathrm{Re} \cdot f^{0.5}}\right) \tag{14}$$

Figs. 5–7 present pressure drop data for smooth, 18° helix, and 0° helix tubes flattened to 0.974 mm high. The pressure drop correlations developed by Jung and Radermacher [3] and Souza et al. [4] predict the pressure drop to within 40%. The correlations used for comparison exhibit the same trends no matter the tube height or internal geometry with Jung and Radermacher [3] giving somewhat higher pressure drop predictions than Souza et al. [4]. The data suggests that standard correlations can be used by determining the smooth tube hydraulic diameter and an equivalent microfin roughness factor.

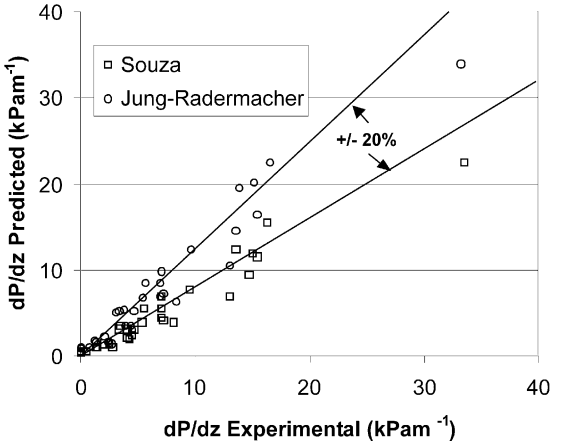

Fig. 5. Comparison of pressure drop predictions of the Souza and Jung–Radermacher correlations with experimental data for a smooth tube flattened to 0.974 mm height.

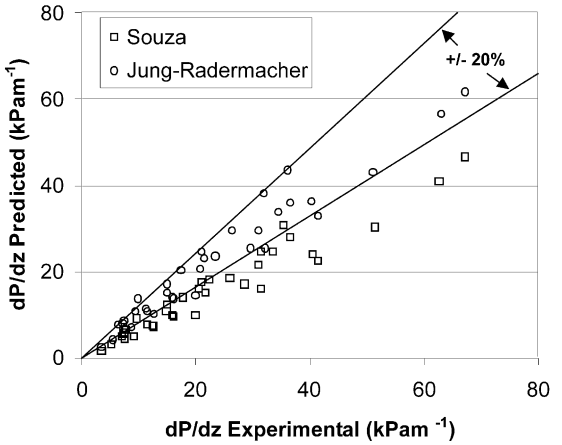

Fig. 6. Comparison of pressure drop predictions of the Souza and Jung–Radermacher correlations with experimental data for an 18° helix tube flattened to 0.974 mm height.

5. Heat transfer coefficients

The third phase of this study examined two-phase refrigerant heat transfer coefficients in the flattened test

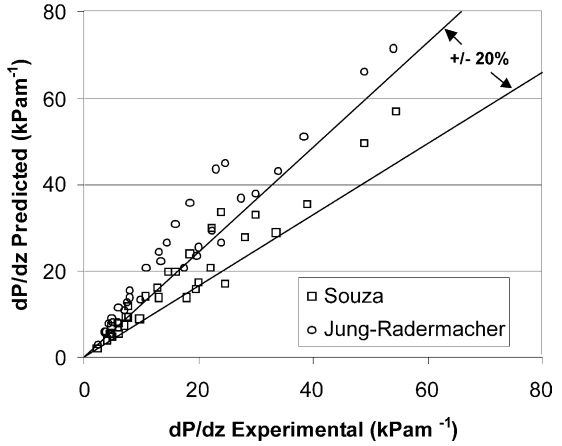

Fig. 7. Comparison of pressure drop predictions of the Souza and Jung–Radermacher correlations with experimental data for a 0° (axially grooved) helix tube flattened to 0.974 mm height.

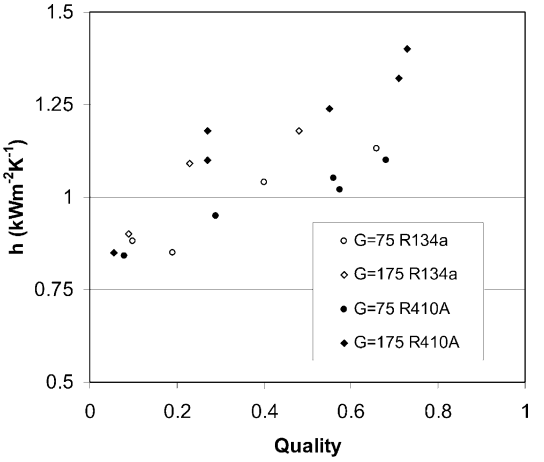

Fig. 8. Condensation heat transfer coefficient data for a 8.91 mm diameter smooth, round tube. Saturation temperature is 35 °C and mass flux (G) is in kg m^{-2} s^{-1}.

sections. As previously described, the local heat transfer coefficient was determined from the water cooling rate and by measuring the local wall and refrigerant temperatures. Inlet and outlet qualities varied between 0.05 and 0.5 with the flattest sections at low mass fluxes resulting in the largest test section quality changes. In each case, the cooling rate and the test section quality was adjusted such that the refrigerant inlet and outlet were in saturation. The average of the inlet and outlet quality is used as the "local" quality in the figures presented.

The heat transfer results display a number of complex trends. Although many investigators have studied refrigerant condensation in round tubes, our understanding of the basic fluid mechanic processes are quite limited [7]. In this study, it is hoped that the successive flattening of an initially round tube minimizes errors that may occur between different test section tubes of varying cross section. That is, the current method was selected in order to have minimal disturbance of wall thermocouples, cooling water flow, test section joints, etc., such that relative changes of heat transfer can be observed as a round tube's cross section profile is continuously altered.

The measured heat transfer coefficients are compared to the round smooth tube heat transfer coefficients at the same mass flux by defining an "enhancement factor".

$$\mathrm{EF} = \frac{(hA_s)}{(hA_s)_{rsG}} \tag{15}$$

The denominator in Eq. (15) represents the heat transfer of a smooth round tube at the same mass flux as the flattened tube. In order to have a consistent basis for predicting the condensation heat transfer of a smooth round tube, several smooth tube heat transfer models were compared to the experimental smooth tube condensation heat transfer results. Varying levels of agreement was found among many popular models [2]. The smooth tube experimental results tended to be consistently lower than the heat transfer coefficients predicted by the Dobson and Chato [8] model by approximately 20–30%. A simple multiplier constant was used to adjust the Dobson and Chato [8] prediction model in order to develop a reference for the enhancement factor calculations, resulting in a smooth round tube enhancement factor of approximately unity for the experimental results collected in this study.

Fig. 8 is a plot of the condensation heat transfer coefficient results for the smooth round tube at two mass fluxes for refrigerants R134a and R410A. Both increasing mass flux and quality tend to increase the heat transfer coefficients as expected. These refrigerants, as well as other halogenated refrigerants in the mid-pressure to high pressure range tend to have similar levels of heat transfer coefficients. R410A has a relatively high liquid thermal conductivity that somewhat compensates for its lower vapor velocity in comparison to R134a. Fig. 9 presents condensation heat transfer coefficient data for the smooth tube flattened to an internal height of 2.57 mm. At mass fluxes equivalent to those in Fig. 8, elevated levels of heat transfer are observed.

The reasons for elevated heat transfer in the flattened tube are unknown, but some speculation concerning the enhancement of heat transfer can be made. First, the lowered height of the tube reduces the energy needed to wet the upper tube surface, possibly causing transition from stratified flow to an annular flow configuration earlier than a round tube. Annular flow tends to have higher rates of heat transfer because the film around the

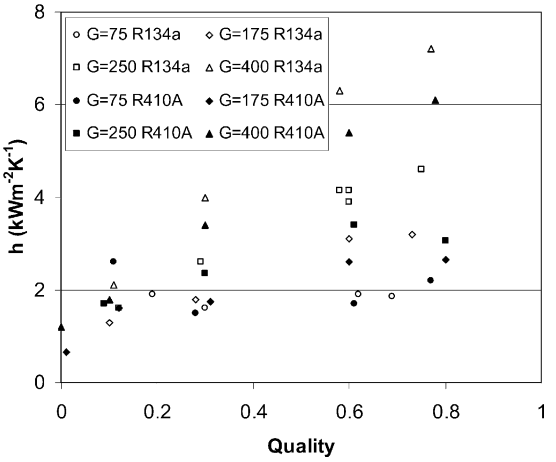

Fig. 9. Condensation heat transfer coefficient data for a smooth tube flattened to an internal height of 2.57 mm. Saturation temperature is 35 °C and mass flux (G) is in kg m^{-2} s^{-1}.

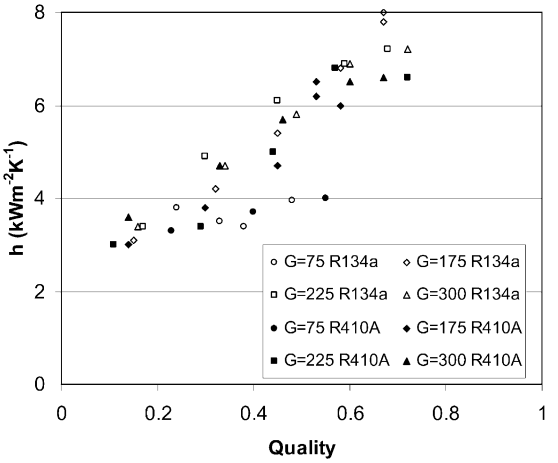

Fig. 10. Condensation heat transfer coefficient data for a 18° helix angle microfin tube flattened to an internal height of 4.15 mm. Saturation temperature is 35 °C and mass flux (G) is in kg m^{-2} s^{-1}.

tube increases the turbulent interaction between the vapor and liquid phases through the "roughness" of the liquid film. Second, the flattened tube may alter the flow field in a manner that increases the heat transfer without changing the flow field configuration. That is, the flow field may be unaltered from a stratified or annular flow configuration, but the flow field within that configuration may be affected. For example, some annular flows have "disturbance wave" or "ring wave" structures while others do not. A third possibility is the formation of a different flow field configuration from that commonly observed in round tubes. Shedd [9] observed interesting liquid wall film thickness variations in non-circular (square, diamond, and triangular cross sections) tubes, apparently caused by the secondary flow field and streamwise flow field variations. In a flattened tube, such flow field variations may also develop. The non-circular shape may also allow the liquid phase to segregate by migrating to one or both of the side regions, with vapor primarily flowing through the center channel region of the tube.

Figs. 10 and 11 present sample condensation heat transfer data for the microfin tubes. Fig. 10 presents results for the 18° helix tube with an internal flattening height of 4.15 mm. A significant jump in heat transfer is observed as the mass flux is increased from a mass flux of 75 kg m^{-2} s^{-1} to the higher mass flux levels. A less prominent change of heat transfer with mass flux increases is observed in the axial tube data for an internal flattening height of 2.57 mm shown in Fig. 11. A study of microfin tube condensation for round 18 degree and axially finned tubes is given by Graham et al. [10]. The local condensation effects of a round, axial finned tube are especially interesting because of localized regions of relatively high enhancement. These effects further complicate the possible nature of the effects displayed by a flattened tube.

Enhancement factors, in combination with heat transfer coefficient information help describe the effects of tube flattening. As previously mentioned, a smooth, round tube is used as the reference case for the flattened tube results. Fig. 12 presents the effect of internal tube flattening height for the smooth tube for two mass fluxes for refrigerants R134a and R410A. Results for Fig. 12 were selected from experiments in which the average quality is 0.3 (±0.05). A trend line is sketched through the data. A peak enhancement in this mass flux range

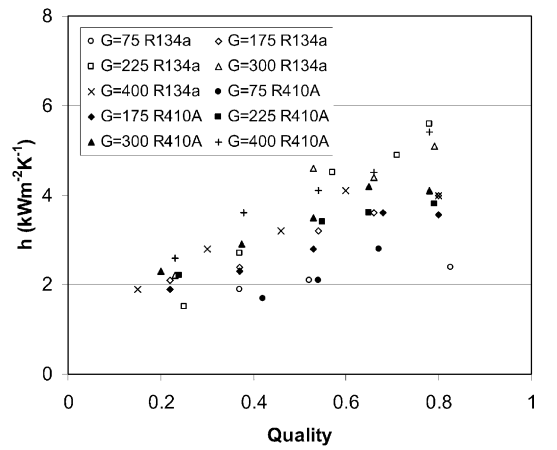

Fig. 11. Condensation heat transfer coefficient data for an axial microfin tube flattened to an internal height of 2.57 mm. Saturation temperature is 35 °C and mass flux (G) is in kg m^{-2} s^{-1}.

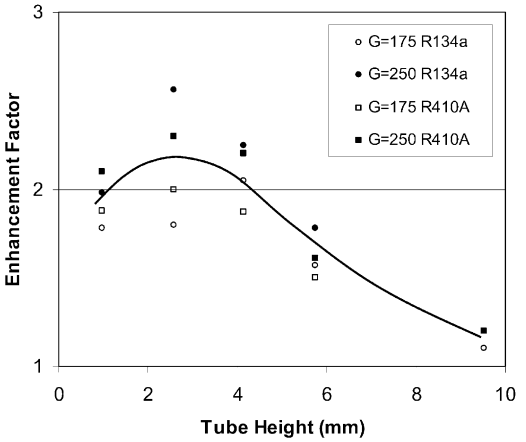

Fig. 12. Enhancement factor versus tube height for a flattened smooth tube at an approximate quality of 0.3. The mass flux (G) is in kg m^{-2} s^{-1}.

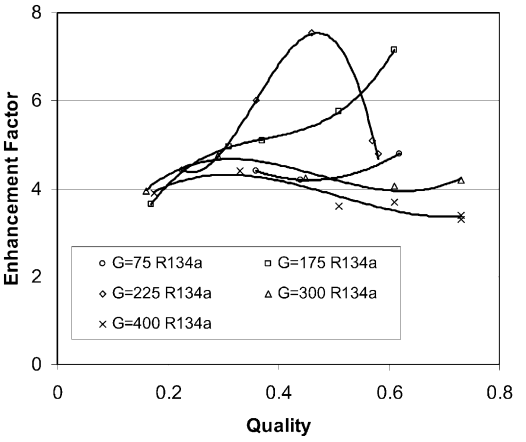

Fig. 14. Heat transfer enhancement factors for R134a in an 18° helix angle tube flattened to 2.57mm over a range of quality and mass flux (mass flux, G, is kg m^{-2} s^{-1}).

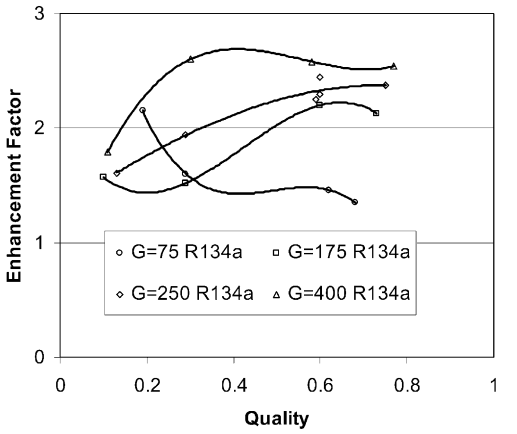

Fig. 13. Heat transfer enhancement factors for R134a in a smooth tube flattened to 2.57 mm over a range of quality and mass flux (mass flux, G, is kg m^{-2} s^{-1}).

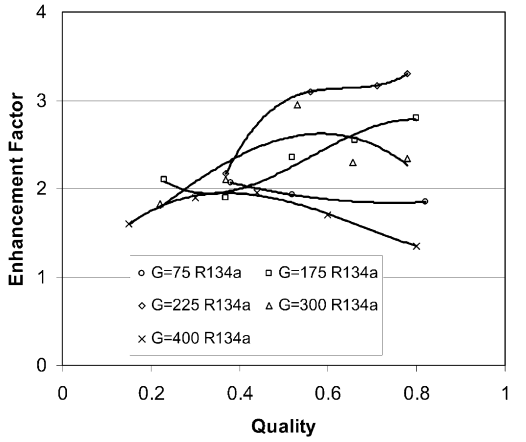

Fig. 15. Heat transfer enhancement factors for R134a in a 0° helix angle tube flattened to 2.57 mm over a range of quality and mass flux (mass flux, G, is kg m^{-2} s^{-1}).

for both refrigerants is observed at approximately 3 mm tube height.

Figs. 13–15 show enhancement factor trends for the smooth tube, 18 degree microfin tube, and axial microfin tube with an internal height of 2.57 mm (near the optimal flattening height observed in Fig. 12 for the smooth tube). For clarity, only results for R134a are shown. Similar effects are observed for R410A. Third order polynomial trendlines have been sketched over each set of mass flux data on the plots in order to help identify changes of heat transfer as the mass flux is varied. The 18° helix microfin tube display significantly higher levels of enhancement over both the smooth and axial microfin tubes. One thought regarding the 18° tube's performance is that as its upper and lower walls are brought closer together, the alternating directions of the microfins cause a favorable distribution of the liquid flow, resulting in an overall thinner average liquid film thickness. An interesting trend observed in each of these figures is the relatively low enhancement factor at the lowest mass flux level, followed by a significant increase of enhancement factor with mass flux. The increase of enhancement factor is also seen to be dependent on quality. Beyond a certain mass flux, however, the enhancement factor in the microfin tubes drops to a fairly steady level. The smooth tube builds to its highest level of enhancement factor at the highest mass flux shown in Fig. 13. It is unknown if the enhancement factor for the smooth tube would begin decreasing if the mass flux were increased beyond the level shown in Fig. 13.

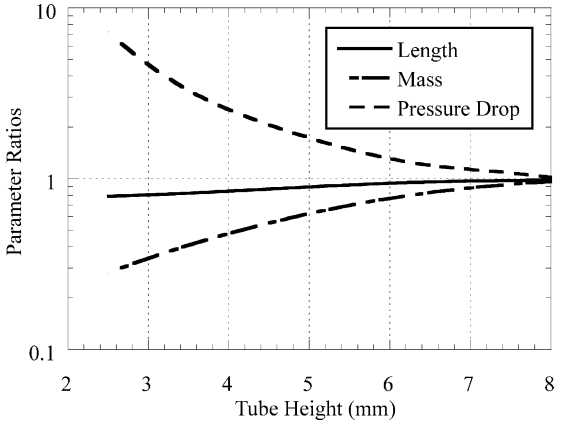

Fig. 16. System simulation prediction results for heat transfer, pressure drop, and charge ratios in a condensing tube circuit as a function of tube height.

6. Combined prediction of charge, pressure drop and heat transfer

The experimental results from the preceding sections can be used to model tubes in a heat exchanger. As an example, a smooth condenser tube with a thermal load capacity of 1750 Watts is modeled. R134a is chosen to be the refrigerant with an inlet temperature of 35 °C. The heat exchanger tube is divided into 100 sections, with each section having a quality change of 1%. Using the average quality in each section, the refrigerant side heat transfer coefficient, pressure drop, and void fraction is calculated. Using the refrigerant side heat transfer coefficient in conjunction with an assumed air-side heat transfer value of 28.0 Wm^{-1} K^{-1} (per unit length of the heat exchanger tube), the length of each section can be determined. Next, the pressure drop and refrigerant mass in the section can be calculated. The properties of each section are then added to determine the length, refrigerant mass, and pressure drop in the heat exchanger circuit.

The results of the smooth tube simulation appear in Fig. 16. In this figure, the changes in pressure drop, refrigerant mass, and tube length (heat transfer area) are compared. These changes are represented as a ratio of the flattened tube heat exchanger characteristics, to the round tube heat exchanger characteristics. As the tube is flattened, the total length of tube required decreases, the total refrigerant mass decays exponentially, and the pressure drop increases exponentially. At a height of 5 mm the pressure drop has increased by 70%, while the total tube length has decreased by 10%, and the amount of refrigerant required has decreased by 40%. The decrease of the length by only 10% is due to the air side being the dominate resistance to heat transfer. The simulation shows similar results for comparisons with microfin tubes. A more accurate model for exploiting the possible benefits of a flattened tube condenser would also consider the variations of the tube flattening on the air side pressure drop and heat transfer.

7. Conclusions

The purpose of this study was to explore the refrigerant side flow characteristics inside of flattened tubes. Some of the findings of flat tubes are:

- Significant reduction in refrigerant mass occur as a tube is flattened
- Pressure drop results scale with hydraulic diameter
- Microfin pressure drop effects can be modeled with equivalent roughness factors
- Heat transfer enhancements are observed as tube profiles are flattened
- 18 helix angle microfin tubes have significantly higher heat transfer than either smooth or axial microfin tubes

The downside of flattening a tube is the increased pressure drop penalty. One possible alternative is to flatten a large tube to increase the hydraulic diameter or to add more parallel circuits. These modifications, however, require more detailed economic considerations by heat exchanger and system manufacturers.

Acknowledgements

The authors appreciate the support of the Copper Development Association and its member companies for providing financial support and guidance.

References

[1] Sacks PS. Measured characteristics of adiabatic and condensing single-component two-phase flow of refrigerant in a 0.377 in. diameter horizontal tube. ASME Winter Annual Meeting, 75-WA/HT-24, 1975.
[2] Wilson MJ, Newell TA Chato JC. A study of two-phase refrigerant behavior in flattened tubes. ACRC report CR-35. Air Conditioning and Refrigeration Center, University of Illinois at Urbana-Champaign, 2001.
[3] Jung DS, Radermacher R. Prediction of pressure drop during horizontal annular flow boiling of pure and mixed refrigerants. Int J Heat Transfer 1989;32(12): 2435–46.
[4] Souza AL, Chato JC, Wattelet JP, Christoffersen BR. Pressure drop during two-phase flow of pure refrigerants and refrigerant-oil mixtures in horizontal smooth tubes.

Heat Transfer with Alternate Refrigerants, ASME HTD 1993;243:35–41.
[5] Cavallini A, Del Col D, Doretti L, Longo GA, Rossetto L. Heat transfer and pressure drop during condensation of refrigerants inside horizontal enhanced tubes. Int J Refrigeration 2000;23:4–25.
[6] Colebrook CF. Turbulent flow in pipes, with particular reference to the transition region between the smooth and rough pipe laws. J of the Institution of Civil Engineers, London 1938–1939;11:133–56.
[7] Newell TA, Shah R. An assessment of refrigerant heat transfer, pressure drop, and void fraction effects in microfin tubes. Int J HVAC&R Research 2000;7(2):125–53.
[8] Dobson MK, Chato JC. Condensation in smooth horizontal tubes. J Heat Transfer 1998;120:193–213.
[9] Shedd TA. Characteristics of the liquid film in horizontal two-phase flow. PhD thesis, University of Illinois at Urbana-Champaign, 2001.
[10] Graham D, Chato JC, Newell TA. Heat transfer and pressure drop during condensation of refrigerant 134a in an axially grooved tube. Int J Heat and Mass Transfer 1999;42:1935–44.